J|A|C|S COMMUNICATIONS

Published on Web 10/21/2010

Oxidation Does Not (Always) Kill Reactivity of Transition Metals: Solution-Phase Conversion of Nanoscale Transition Metal Oxides to Phosphides and Sulfides

Elayaraja Muthuswamy and Stephanie L. Brock*

Department of Chemistry, Wayne State University, Detroit, Michigan 48202, United States

Received July 19, 2010; E-mail: sbrock@chem.wayne.edu

Abstract: Unexpected reactivity on the part of oxide nanoparticles that enables their transformation into phosphides or sulfides by solution-phase reaction with trioctylphosphine (TOP) or sulfur, respectively, at temperatures of ≤370 °C is reported. Impressively, single-phase phosphide products are produced, in some cases with controlled anisotropy and narrow polydispersity. The generality of the approach is demonstrated for Ni, Fe, and Co, and while manganese oxides are not sufficiently reactive toward TOP to form phosphides, they do yield MnS upon reaction with sulfur. The reactivity can be attributed to the small size of the precursor particles, since attempts to convert bulk oxides or even particles with sizes approaching 50 nm were unsuccessful. Overall, the use of oxide nanoparticles, which are easily accessed via reaction of inexpensive salts with air, in lieu of organometallic reagents (e.g., metal carbonyls), which may or may not be transformed into metal nanoparticles, greatly simplifies the production of nanoscale phosphides and sulfides. The precursor nanoparticles can easily be produced in large quantities and stored in the solid state without concern that "oxidation" will limit their reactivity.

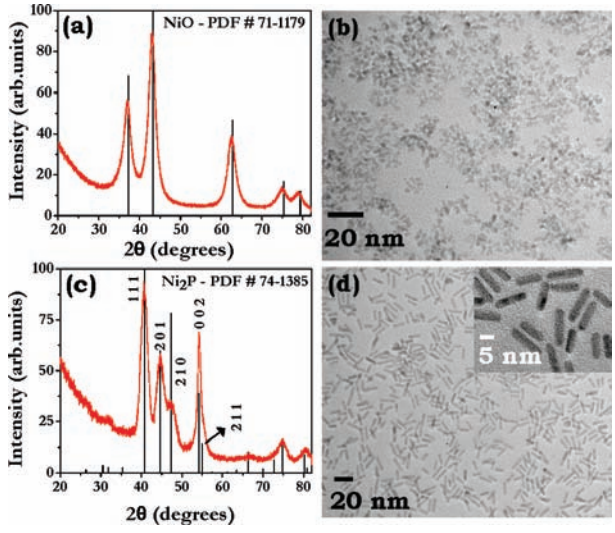

Figure 1. (a, c) PXRD patterns of (a) NiO nanoparticles and (c) Ni_2P nanorods with comparisons to their reference patterns (powder diffraction files) from the ICDD database. (b, d) TEM images of (b) 3−5 nm NiO nanoparticles and (d) 17.9 ± 2.6 nm × 4.0 ± 0.3 nm Ni_2P nanorods.

Transition metal phosphides exhibit a rich and varied range of physical properties resulting in their exploitation in diverse applications such as thermoelectrics and catalysis.[1] The promise of improved properties has led to an emphasis on the preparation of these materials in nanoscale forms.[2] Reported strategies for the synthesis of transition metal phosphide nanomaterials include solvothermal reactions,[3] decomposition of organometallic reagents in the presence of phosphines,[4] decomposition of single-source precursors,[5] high-temperature hydrogen reduction of nanoscale phosphates,[6] and sonochemical synthesis.[7] Schaak and co-workers described the use of trioctylphosphine (TOP) as a general precursor for converting transition metal nanoparticles into phosphides,[8] an approach we have exploited for the rational synthesis of phase-pure phosphides of Fe and consequential elucidation of their intrinsic magnetic properties.[9] A limitation of this approach is the reported lack of reactivity of oxides toward TOP,[8b] because surface oxidation is endemic among most transition metal nanoparticles. Here we show not only that surface oxidation is no impediment to phosphide formation but also that even completely oxidized particles can be converted to phosphides using TOP. Moreover, this reaction is capable of generating phase-pure products in solution at temperatures of ≤370 °C, and in some cases, the particles are highly uniform and even adopt anisotropic morphologies. The conditions that must be met for successful conversion and the extension of this method to sulfides will be highlighted.

Metal oxide nanoparticles (NiO, Fe_3O_4, CoO, Mn_3O_4) were prepared by decomposition of metal acetylacetonate salts in an octylether/oleylamine solvent/surfactant system at 250 °C for 2−3 h under a flow of air. The oxide nanoparticles were isolated by precipitation with excess ethanol followed by centrifugation. The isolated nanoparticles were characterized by powder X-ray diffraction (PXRD) and transmission electron microscopy (TEM) before they were subjected to reaction with TOP.

In the case of Ni, the PXRD pattern was found to be a perfect match to the reference pattern of NiO (Figure 1a). No additional peaks were observed, suggesting that few or no crystalline impurities were present. Moreover, the room-temperature magnetic susceptibility was field-independent, confirming the absence of unreacted Ni (Figure S1 in the Supporting Information). TEM images revealed the formation of nanoparticles with roughly spherical morphology and sizes in the 3−5 nm range (Figure 1b). This is consistent with the size obtained by Scherrer analysis of the PXRD pattern (4.4 nm), suggesting that the particles were fully crystalline. The free-flowing dry NiO nanoparticles were then combined with 10 mL of octylether and 2 mL of oleylamine, degassed under vacuum at 100 °C for 15−20 min, and then heated to 300 °C under argon. TOP (15 mL) was injected into the system, and then the temperature was raised to 350 °C. The system was left at 350 °C for 2−3 h, during which time the color of the solution turned from the characteristic brown of NiO to black. Isolation of the final product was carried out by precipitation with excess ethanol followed by centrifugation.

The PXRD pattern of the product of NiO with TOP (Figure 1c) suggested complete conversion to Ni_2P. There was no evidence of

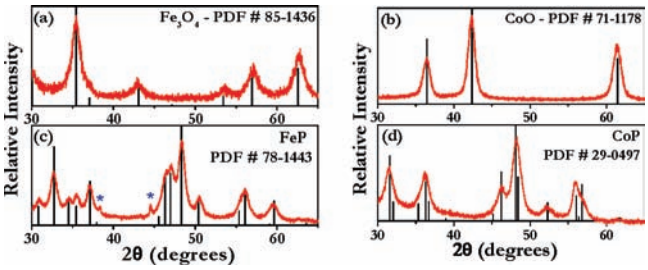

Figure 2. PXRD patterns of (a) Fe_3O_4 nanoparticles, (b) CoO nanoparticles, (c) FeP nanoparticles, and (d) CoP nanoparticles, all compared with their reference patterns. * indicates peaks from the sample holder.

residual oxide or any other nickel phosphide phase. Additionally, relative to the other peaks in the pattern, the (002) reflection was found to be sharp and the (210) reflection broad, suggesting that the particles have a preferred direction of growth along the *c* axis.[4c] The formation of rods was confirmed by TEM analysis (Figure 1d and Figure S2), and electron-dispersive spectroscopy (EDS) data were in agreement with the expected Ni/P ratios (Figure S2). The formation of nanorods indicates that the reaction of NiO with TOP is not topotactic but probably arises from dissolution of the oxide, with the anisotropy being exhibited as a consequence of a high constant concentration of Ni obtained from NiO and the hexagonal symmetry of the crystal structure.[10] This new method of producing nanorods does not require continuous controlled injection of precursors[4b,c,10b] or the use of multiple ligands with different binding strengths[11] to promote the formation of rods/wires. Moreover, it is possible to adjust the aspect ratio of the nanorods by varying the NiO concentration. Thus, increasing concentration 3-fold led to a corresponding increase in aspect ratio (Figure S3).

Reactivity toward TOP is not limited to NiO. However, conversion of Fe_3O_4 nanoparticles (4−7 nm; Figure 2a and Figure S4a) and CoO nanoparticles (8−12 nm; Figure 2b and Figure S5a) using TOP over 4 h at 350 °C resulted in a mixture of phases (Figure S6). Like Ni, the metal (M)-rich M_2P phases were favored, but these were accompanied by significant quantities of the MP phases. In an attempt to prepare phase-pure products, the heating time was extended to 24 h, and in the case of Co, the temperature was raised to 370 °C. Phase-pure MP was obtained in both cases, as indicated by PXRD (Figure 2c,d). The formation of the less-metal-rich phase at longer times and higher temperatures is consistent with our previous work on the Fe-to-Fe_xP_y nanoparticle transformation.[9] TEM analyses of the final products indicated that the FeP nanoparticles were present as clumps with diameters of up to 50 nm (Figure S4), whereas CoP nanoparticles formed as discrete particles with size comparable to that of the CoO precursor (Figure S5).

Intriguingly, oxide nanoparticle conversion does not seem to be a universal process. Attempts to convert Mn_3O_4 nanoparticles into a phosphide phase by reaction with TOP were unsuccessful. While TOP reduced Mn_3O_4 nanoparticles to MnO, there was no evidence of phosphide formation (Figure S7). The greater barrier for phosphide generation with Mn has been attributed to its low electronegativity relative to later transition metals.[12]

In order to test the effect of size on the conversion of oxides to phosphides, control reactions were carried out by treating a sample of bulk NiO with TOP. The PXRD pattern of the product clearly indicated that the bulk sample remained principally oxide (Figure S8a). However, when a polydisperse sample of NiO nanoparticles with sizes of ≤50 nm was treated with TOP for 24 h at 385 °C, the product was found to be a mixture of NiO and Ni_2P (Figure S8b). These observations lead us to conclude that the transformation of oxide to phosphide is related to solubility or reactivity of the oxide nanoparticles, each of which is augmented at small particle sizes.

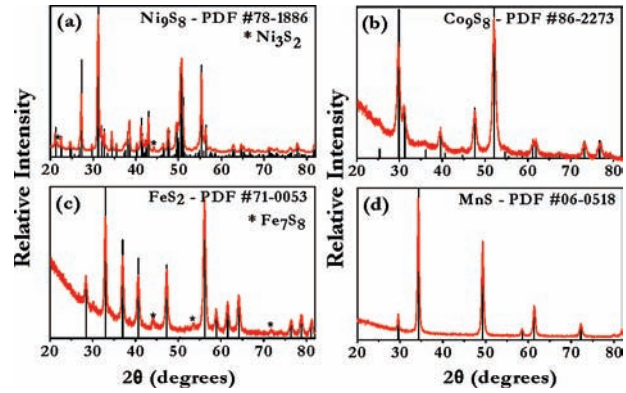

Figure 3. PXRD patterns of (a) MnS nanoparticles, (b) FeS_2 nanoparticles, (c) Co_9S_8 nanoparticles, and (d) Ni_9S_8 nanoparticles, all compared to their reference patterns. * indicates peaks due to minor phases [Ni_3S_2 in (a) and Fe_7S_8 in (c)].

In principle, transition metal sulfides should be even easier to prepare from oxides. Indeed, the oxide-to-sulfide nanoparticle transformation has been reported for conversion of Nd_2O_3 nanoparticles into phase-pure NdS_2 using a mixture of boron and sulfur powders at 450 °C in vacuum-sealed tubes.[13] Accordingly, we tested the applicability of our oxide conversion method to the formation of transition metal sulfides. The PXRD pattern of the product of NiO nanoparticles with sulfur in the presence of oleylamine and octylether at 300−350 °C (Figure 3a) indicates the successful transformation into Ni_9S_8 (major) and Ni_3S_2. Co and Fe oxides were also successfully transformed under similar reaction conditions, producing phase-pure Co_9S_8 (Figure 3b) and a mixed-phase sample of FeS_2 (major) and Fe_7S_8 (Figure 3c), respectively. Intriguingly, although MnO was not reactive toward TOP, it also combined with sulfur to form single-phase MnS (Figure 3d).

These results clearly demonstrate that oxidation does not preclude nanoparticle conversion to phosphides, provided the samples are small enough to dissolve (ca. 10 nm) and that the metal oxides are reactive (Fe, Co, Ni). Moreover, the low rate of reactant introduction and the high local concentration can enable shape anisotropy to be accessed and controlled. Oxides are even more reactive toward sulfur, yielding sulfides even in cases where the corresponding phosphides cannot be produced (e.g., with Mn). Overall, the use of oxide nanoparticles, which are easily accessed via reaction of inexpensive salts with air, in lieu of organometallic reagents (e.g., metal carbonyls), which may or may not be transformed into metal nanoparticles, greatly simplifies the production of nanoscale phosphides and sulfides. The precursor nanoparticles can be produced in large quantities and stored in the solid state without concern that "oxidation" will limit their reactivity.

Acknowledgment. This work was supported by the National Science Foundation (DMR-331769). We thank A. Dixit and G. Lawes for the magnetic data.

Supporting Information Available: Experimental procedures for synthesis and characterization; additional PXRD patterns, TEM images, and EDS and magnetic data. This material is available free of charge via the Internet at http://pubs.acs.org.

References

(1) Hullinger, F. *Struct. Bonding (Berlin)* **1968**, *4*, 83–229.
(2) (a) Brock, S. L.; Perera, S. C.; Stamm, K. L. *Chem.—Eur. J.* **2004**, *10*, 3364–3371. (b) Brock, S. L.; Senevirathne, K. *J. Solid State Chem.* **2008**, *181*, 1552–1559.
(3) Luo, F.; Su, H.-L.; Song, W.; Wang, Z.-M.; Yan, Z.-G.; Yan, C.-H. *J. Mater. Chem.* **2004**, *14*, 111–115.
(4) (a) Perera, S. C.; Fodor, P. S.; Tsoi, G. M.; Wenger, L. E.; Brock, S. L. *Chem. Mater.* **2003**, *15*, 4034–4038. (b) Park, J.; Koo, B.; Yoon, K. Y.; Hwang, Y.; Kang, M.; Park, J.-G.; Hyeon, T. *J. Am. Chem. Soc.* **2005**, *127*, 8433–8440. (c) Park, J.; Koo, B.; Hwang, Y.; Bae, C.; An, K.; Park, J.-G.; Park, H.; Hyeon, T. *Angew. Chem., Int. Ed.* **2004**, *43*, 2282–2285.
(5) Kelly, A. T.; Rusakova, I.; Ould-Ely, T.; Hofmann, C.; Lüttge, A.; Whitmire, K. H. *Nano Lett.* **2007**, *7*, 2920–2925.
(6) Stamm, K. L.; Garno, J. C.; Liu, G.-y.; Brock, S. L. *J. Am. Chem. Soc.* **2003**, *125*, 4038–4039.
(7) Sweet, J. D.; Casadonte, D. J., Jr. *Ultrason. Sonochem.* **2001**, *8*, 97–101.
(8) (a) Henkes, A. E.; Vasquez, Y.; Schaak, R. E. *J. Am. Chem. Soc.* **2007**, *129*, 1896–1897. (b) Henkes, A. E.; Schaak, R. E. *Chem. Mater.* **2007**, *19*, 4234–4242.
(9) Muthuswamy, E.; Kharel, P. R.; Lawes, G.; Brock, S. L. *ACS Nano* **2009**, *3*, 2383–2393.
(10) Chen, Y.; She, H.; Luo, X.; Yue, G.-H.; Peng, D.-L. *J. Cryst. Growth* **2009**, *311*, 1229–1233.
(11) Gregg, K. A.; Perera, S. C.; Lawes, G.; Shinozaki, S.; Brock, S. L. *Chem. Mater.* **2006**, *18*, 879–886.
(12) Gopalakrishnan, J.; Pandey, S.; Rangan, K. K. *Chem. Mater.* **1997**, *9*, 2113–2116.
(13) Wu, L.-M.; Sharma, R.; Seo, D.-K. *Inorg. Chem.* **2003**, *42*, 5798–5800.

JA106397B